Materials Science Forum
ISSN: 1662-9752, Vol. 815, pp 401-406
doi:10.4028/www.scientific.net/MSF.815.401
© 2015 Trans Tech Publications, Switzerland
Online: 2015-03-20

Fabrication and Characteristics of Gene-delivering Nanodevices Based on Au-Ag@CS-FA Hybrid Particles

Qingwen Guan[a] and Min Wang[b*]

Department of Mechanical Engineering, The University of Hong Kong, Pokfulam Road, Hong Kong

[a]anna_guan@hku.hk, [b]memwang@hku.hk

Keywords: Au-Ag nanoparticle, Chitosan, Folic Acid, Hybrid Nanoparticle, Gene delivery.

Abstract. Gene therapy has great potential in offering highly promising treatments for cancer. Polymer-metal hybrid nanoparticles (NPs) are good candidates as gene delivery vehicles due to their unique properties and facile functionalization. The polymer component in hybrid NPs can provide accurate cancer cell targeting and high DNA binding ability while the metallic component can provide imaging functions for the nanodevices. In the present study, hybrid NPs comprising an Au-Ag bimetallic core and a folic acid-chitosan shell (Au-Ag@CS-FA) were fabricated. The structure and relevant properties of Au-Ag@CS-FA NPs were subsequently studied using a variety of techniques， like scanning electron microscope (SEM), Fourier transform infrared spectroscopy (FTIR), transmission electron microscope (TEM) and UV-visible spectra. Their DNA binding ability was also assessed. Results showed that Au-Ag@CS-FA NPs possessed properties that can make them excellent gene delivery vehicles.

Introduction

Gene therapy, which uses exogenous genes to perform therapeutic functions, holds great promises for cancer treatment. Therapeutic genes can be delivered to replace defective genes which cause diseases or silence the expression of mutated genes. The success of gene therapy depends on delivery vectors because it is hard for naked therapeutic genes to cross extracellular barriers and subsequently be transfected [1]. Although viral vectors have been most frequently employed due to their high transfection efficiency, safety concerns rising from insertional mutagenesis and immune responses make non-viral vectors preferable over viral vectors. Nanotechnology now offers unprecedented opportunities to explore potential non-viral vectors based on nanoparticles (NPs). One approach involves the utilization of biodegradable cationic liposomes or polymers comprising amino groups, such as chitosan, poly l-lysine (PLL), polyethyleneimine (PEI) and gelatin [2], which could bond with phosphate groups of DNA via electrostatic interaction. Another approach focuses on inorganic nanoparticles whose nanoscale characteristics in terms of small size and high surface-to-volume ratio enable maximum gene payloads to carrier ratio. Among these inorganic NPs, gold NPs show promises for gene delivery due to their good biocompatibility and facile functionalization [3]. The modification of surface charge and hydrophobicity could maximize transfection efficiency while minimize toxicity. Ghosh et al. [4] developed gold NPs (AuNPs) that effectively bind with pDNA by directly conjugating cationic amino acid ligands on the surface of AuNPs. Thomas and Klibanov [5] functionalized AuNPs with branched PEI to provide hybrid AuNP-polymer delivery vehicles, which showed 12-fold higher transfection efficiency than their polymer counterparts. Chitosan-capped gold nanospheres demonstrated enhanced DNA binding and stability without compromising DNA release [6]. Although these hybrid polymer-gold nanodevices have demonstrated the general applicability of AuNPs in gene delivery, in some cases the NP/DNA complex seemed to aggregate due to their micrometer size. The distinct optical and electromagnetic properties of gold component in nanodevices have also been significantly lowered. Nanodevices lacking the targeting ability could result in low cellular internalization. These problems have restricted the development of AuNPs and similar NPs as useful non-viral vectors. In the present study, novel core-shell structured hybrid nanoparticles in which a highly branched Au-Ag bimetallic core was coated by a folic acid modified chitosan shell (Au-Ag@CS-FA) were synthesized and evaluated. The cationic polyelectrolyte nature of the polymer shell could provide a strong electrostatic interaction with negatively charged DNA and protect it from nuclease degradation. Folic acid was conjugated to chitosan for increasing the transfection efficiency and also for targeting cancer cells. CS-FA conjugates were also used as reducing and structure-directing agent during the formation of the Au-Ag core. The bimetallic core would exhibit strong surface plasmon-enhanced absorption and scattering ability, providing the capability for optical imaging.

Materials and Methods

Materials. Chloroauric acid, silver nitrate ($AgNO_3$), L-ascorbic acid (AA), folic acid (FA), hydroxysuccinimide (NHS), 3-(ethyliminomethyleneamino)-N,N-dimethyl-propan-1-amine (EDC), Tris Acetate-EDTA buffer, low molecular weight chitosan, acetic acid, agarose powder, gel loading buffer solution, ethidium bromide solution and other raw materials/chemicals were supplied by Sigma-Aldrich, USA. All solutions were prepared by using de-ionized (DI) water from Millipore (Model Milli-Q, USA).The plasmid DNA which encoded the enhanced green protein with a CMV promoter was supplied by the Department of Pathology, The University of Hong Kong.

Synthesis of FA-conjugated chitosan. The conjugation of folic acid to chitosan was based on the EDC/NHS coupling reaction. A solution of EDC, NHS and FA in anhydrous dimethyl sulfoxide (DMSO) was prepared and stirred for 12 h. The solution was then added dropwise to a 1% (w/v) chitosan solution in acetate buffer and continuously stirred for 16 h. The resulting mixture was adjusted to pH 9.0 and dialyzed against phosphate buffer (pH 7.4) for 24 h and then against water for 48 h. The polymer was isolated by lyophilization and the powder obtained was collected for further analysis and use.

Fabrication of Au-Ag@CS-FA nanoparticles. Au-Ag@CS-FA NPs were synthesized according to our previously established procedure [7]. A CS-FA solution (0.5 mg/ml in 1% acetic acid) was mixed with a $HAuCl_4$ aqueous solution (1 mM) under vigorously stirring for half an hour. Then an $AgNO_3$ solution (0.01 M) was added, followed by the addition of AA solution (0.1 M) and the mixture was continuously stirred for another 2-3 h. The products were collected by centrifugation, washed three times with DI water and 1% acetic acid, and finally dispersed in DI water.

Folic acid content of CS-FA conjugates. The content of FA in CS-FA conjugates was calculated based on the standard curve obtained from an UV-vis spectrometer (UV2600, Shimadzu, Japan). FA and CS-FA were dissolved in acetate buffer (pH 5.8). CS-FA solution of 0.5 mg/L and FA solution of 0.01-0.15 mg/L were prepared. Absorbance spectra of FA solution at different concentrations from 250-400 nm were obtained using the UV-vis spectrometer. The absorbance values of the peak intensities at 362 nm of the absorbance spectra were analyzed as a function of FA concentration. The absorbance value of the peak density at 362 nm of CS-FA was also obtained. The concentration of FA in CS-FA was calculated according to the Beer-Lamber's law and the content of FA was thus calculated for Au-Ag@CS-FA NPs.

Formation of the Au-Ag@CS-FA/pDNA complex. The Au-Ag@CS-FA/pDNA complex was made using a complex coacervation technique [8]. Au-Ag@CS-FA NPs were dispersed in deionized water to form a suspension (1 mM). A plasmid DNA stock solution (860 ng/µL) was prepared using deionized water. The NPs suspension and DNA stock solution were mixed and stirred to form Au-Ag@CS-FA/pDNA complex with different molar ratios of NPs/pDNA. To study the effect of pH on the binding ability of NPs, one part of mixture was added by 1% acetic acid and was adjusted to pH 5.8, the other was added with the same amount of deionized water as control. Both of them were incubated at 37 °C for half hour. Electrophoresis was carried out in 1% (w/v) agarose gel at 80 V for half hour. After staining, the DNA localization in gel was visualized using a UV lamp.

Characterization. The particle size and zeta potential of NPs synthesized were measured using dynamic light scattering (DLS, DelsaNano C, Beckman Counter, Canada). The morphology and structure of NPs were studied using SEM (S4800, Japan) and TEM (CM100, Philips, the Netherlands). The chemical composition of FA, CS, and CS-FA were characterized using FTIR spectrometry (Spectrum BX, Perkin Elmer, USA).

Results and Discussion

Folic acid-chitosan conjugation. FA was conjugated to CS molecules through the reaction of carboxyl groups of FA with amino groups of CS under EDC/NHS catalysis. The FTIR spectra of FA, CS and CS-FA conjugate, are shown in Fig. 1. Characteristic absorption peaks of FA at 1412 cm^{-1} and 1603 cm^{-1}, which corresponded to the stretching vibration of C=C backbone of aromatic ring on FA, were also observed in the spectrum for CS-FA conjugate. The absorption peak at 1570 cm^{-1} in the spectrum for CS-FA conjugate, was attributed to bonded N-H (amide II band) of newly formed -CONH- groups, whereas the peak at 1656 cm^{-1} for the $-NH_2$ bending vibration of CS weakened greatly. These results confirmed that FA was successfully conjugated into CS.

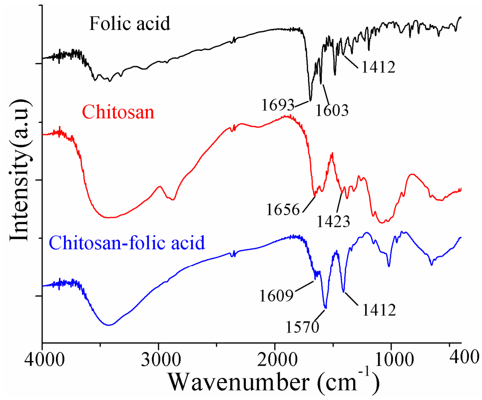

Fig. 1 FTIR spectra of folic acid (FA), chitosan (CS) and CS-FA conjugate

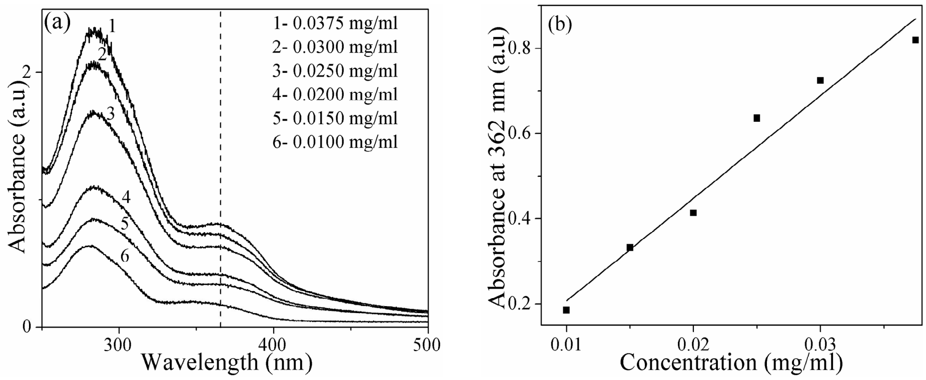

Fig. 2 (a) UV spectra of FA solutions with known FA concentrations. (b) Linear relationship between FA concentration (mg/mL) and absorbance at 362 nm on UV spectra.

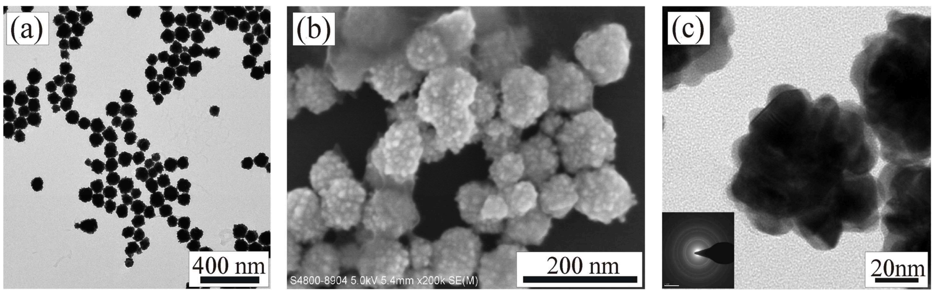

Fig. 3 Morphology and microstructure of bimetallic Au-Ag NPs. (a) TEM image of Au-Ag NPs (low magnification). (b) SEM image of Au-Ag NPs. (c) TEM image of Au-Ag NPs (high magnification) with an inset for the SAED pattern

Characterization of nanoparticles. Bimetallic NPs have drawn increasing attention because of the possibility to tune the composition to optimize their optical and electronic properties. The Au-Ag bimetallic NPs with superior optical properties have thus been intensively studied. Two main groups of Au-Ag bimetallic NPs, namely, the alloyed and the layered (core-shell) NPs, can be prepared by simultaneous co-reduction or by successive reduction of one metallic on the nuclei of the other. Compared to simultaneous co-reduction, the latter method provides better control of the morphology and chemical contents of resultant NPs. In the present study, the synthesis of Au-Ag bimetallic NPs were performed through the succesive layer-by-layer deposition of Au and Ag. The synthesized Au-Ag NPs had the well-defined highly branched shape with a solid core and sharp branches, having the size around 90 nm, as shown in Fig. 3. The inset in Fig. 3c is a selected area electron diffraction (SAED) pattern which indicated that NPs were cystalline material with random oriention. High resolution TEM image (Fig. 3c) showed the highly branched structure. A rough particle surface observed through SEM and TEM indicated that the NPs could generate strong collective surface plasmon resonances for local electromagnetic enhancement, which subsequently increase the intensity of Raman molecules embedded in nanodevices. These results made the Au-Ag NPs useful as a surface-enhanced Raman scattering (SERS) tag for cancer cell imaging. Since the reagent used in the particle synthesis processes are non-toxic, the synthesized NPs can be readily integrated with biomolecules.

Fig.4 shows that the average hydrodynamic diameter of Au-Ag NPs was approximately 100 nm and their zeta potential was +37.1 mv in deionized water, suggesting that the cationic nature of nanoparticles which could provide bonding with negatively charged DNA. The DLS results revealed that the NPs were monodispersed with a narrow size distribution, ensuring their high stability in the physical-chemical environment. In addition, their nanosized features could facilitate their accumulation in tumor tissue via Enhanced permeability and retention (EPR) effects for passive targeting.

The main surface plasmon resonance (SPR) absorption peak of Au-Ag@CS-FA NPs appeared at around 560 nm in UV-Vis spectra (Fig. 5b), which is located in the visible light region. The absorption peaks at 280 nm and 362 nm were attributed to the CS-FA conjugate, as FA has three typical broad absorption peaks at 255 nm, 283 nm and 365 nm. According to TEM examination, a thin polymer shell with a thickness of about 5 nm was present on the Au-Ag core (Fig. 5a), which not only contributed to the monodispersed nature of Au-Ag@CS-FA NPs but also could be used subsequently for binding with DNA.

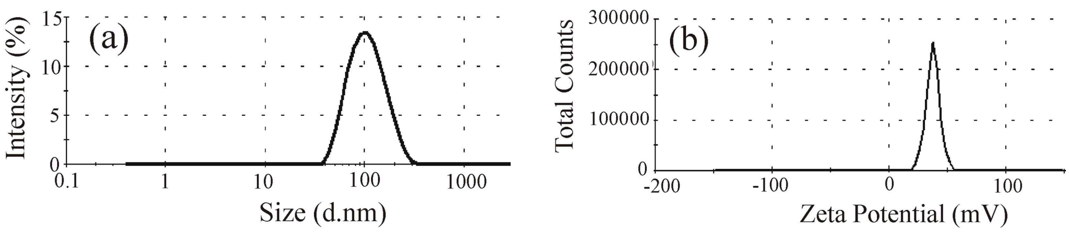

Fig. 4 Characteristics of Au-Ag NPs. (a) Particle size distribution. (b) Zeta potential.

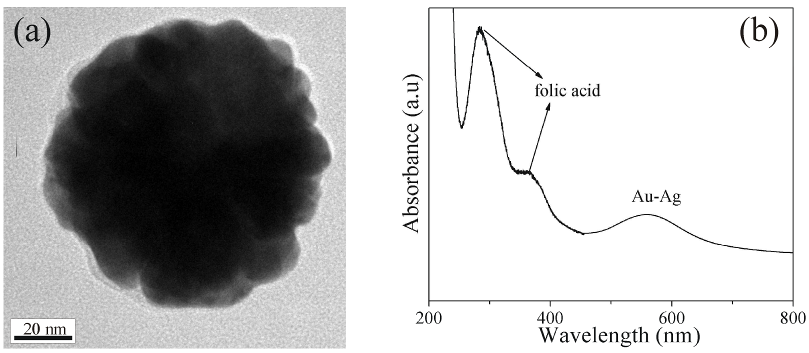

Fig. 5 (a) TEM images of Au-Ag@CS-FA nanoparticles shows a thin polymer shell. (b) UV-vis spectra of Au-Ag@CS-FA NPs

Physico-chemical properties of Au-Ag@CS-FA hybrid NPs and NP/pDNA complexes. Plasmid DNA and Au-Ag@CS-FA NPs at different molar ratios were subjected to agarose gel electrophoresis to characterize the formation process of NP/pDNA complexes. Free pDNA was observed in Fig. 6 as two fluorescent bands corresponding to the supercoiled and circular forms of the plasmid. When pDNA was combined with Au-Ag@CS-FA NPs at low NP/pDNA ratio, a fraction of plasmid DNA was free to migrate into gel (as shown in Fig. 6a, lane 2-4). The binding ability of plasmid DNA with NPs under either neutral or acidic pH was studied. With NP:pDNA molar ratio from 1:1 up to 10:1, no successful retardation of pDNA was found when mixture of NPs and pDNA were suspended and incubated in neutral medium (Fig. 6a). However, the complete retardation of pDNA was achieved at a NP/pDNA ratio of 10:1 when the mixture was incubated in the acidic medium (Fig. 6b), indicating that the condensation of plasmid DNA by Au-Ag@CS-FA NPs was feasible in the acidic condition. In other words, the acidic condition could uplift the binding ability of Au-Ag@CS-FA NPs. This can be attributed to the enhanced protonation of amino groups in the CS-FA layer on Au-Ag@CS-FA NPs. Compared to previous work by others [4, 5], our Au-Ag@CS-FA NPs exhibited higher DNA condensing efficiency due to their relative large surface area and more cationic polymer coating. Further work is currently conducted to optimize the DNA condensing ability by modifying the conjugation of folic acid to chitosan.

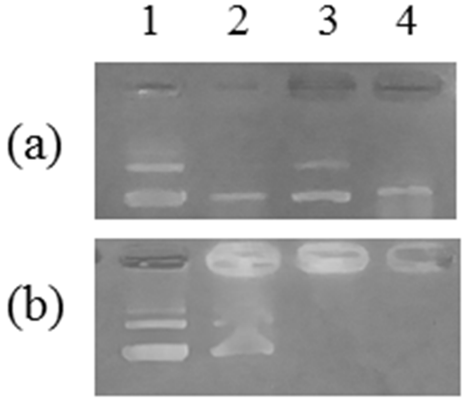

Fig. 6 Electrophoresis mobility analysis of pDNA and NP/pDNA complexes on a 0.5% agarose gel stained with ethidium bromide: (a) NP/pDNA incubated in the neutral medium(Lane 1: naked plasmid DNA; Lane 2 to 4: the molar ratio of NP to pDNA was 1:1, 5:1, 10:1, respectively); (b) NP/pDNA complexes incubated in the acidic medium (pH 5.8). (Lane 1: naked plasmid DNA; Lane 2 to 4: the molar ratio of NP to pDNA was 5:1, 10:1, 20:1, respectively.

Conclusions

The hybrid polymer-metal NPs as potential gene delivery vehicles are synthesized using a facile method. The Au-Ag@CS-FA NPs based on highly branched bimetallic Au-Ag NPs are stable with good biocompatibility and strong DNA binding ability in the acidic condition. FA molecules are conjugated onto CS and the CS-FA conjugate forms a thin shell on the Au-Ag core in hybrid NPs. Au-Ag@CS-FA NPs show great promise as a new gene delivery vehicle.

Acknowledgements

This work was supported by a research grant from The University of Hong Kong in its Basic Research Program and a GRF grant (HKU 7177/13E) from the Research Grants Council of Hong Kong. Q.-W. Guan thanks The University of Hong Kong for providing her with a research studentship. Dr. S.-Y. Li's assistance is acknowledged.

References

[1] I.M. Verma, N. Somia, Gene therapy-promises, problems and prospects, Nature. 389 (1997) 239-242.

[2] M. Thomas, A. Klibanov, Non-viral gene therapy: polycation-mediated DNA delivery, Appl. Microbiol. Biot. 62 (2003) 27-34.

[3] P. Ghosh, G. Han, M. De, C.K. Kim, V.M. Rotello, Gold nanoparticles in delivery applications, Adv. Drug. Deliv. Rev. 60 (2008) 1307-1305.

[4] P.S. Ghosh, C.-K. Kim, G. Han, N.S. Forbes, V.M. Rotello, Efficient gene delivery vectors by tuning the surface charge density of amino acid-functionalized gold nanoparticles, Acs. Nano. 2 (2008) 2213-2218.

[5] M. Thomas, A.M. Klibanov, Conjugation to gold nanoparticles enhances polyethylenimine's transfer of plasmid DNA into mammalian cells, Proc. Natl. Acad. Sci. 100 (2003) 9138-9143.

[6] X. Zhou, X. Zhang, X. Yu, X. Zha, Q. Fu, B. Liu, X. Wang, Y. Chen, Y. Chen, Y. Shan, The effect of conjugation to gold nanoparticles on the ability of low molecular weight chitosan to transfer DNA vaccine, Biomaterials. 29 (2008) 111-117.

[7] S.Y. Li, M.Wang, A Novel SERS-Active Tag Based on Bimetallic Flowerlike Au-Ag Nanoparticles, Curr. Nanosci. 7 (2011) 969-978.

[8] S. Mansouri, Y. Cuie, F. Winnik, Q. Shi, P. Lavigne, M. Benderdour, E. Beaumont, J.C. Fernandes, Characterization of folate-chitosan-DNA nanoparticles for gene therapy, Biomaterials. 27 (2006) 2060-2065.

[9] M. Stevanović, A. Radulović, B. Jordović, D. Uskoković, Poly (DL-lactide-co-glycolide) nanospheres for the sustained release of folic acid, J. Biomed. Nanotechnol. 4 (2008) 349-358.

[10] Z. Zhang, J. Jia, Y. Lai, Y. Ma, J. Weng, L. Sun, Conjugating folic acid to gold nanoparticles through glutathione for targeting and detecting cancer cells, Bioorgan. Med. Chem. 18 (2010) 5528-5534.